SLOW-TIME MULTI-FREQUENCY RADAR FOR TARGET DETECTION IN MULTIPATH SCENARIOS

Satyabrata Sen and Arye Nehorai

Department of Electrical and Systems Engineering,
Washington University in St. Louis,
St. Louis, MO 63130, USA.
e-mail: {ssen3, nehorai}@ese.wustl.edu.

ABSTRACT

We propose a method to detect a target in the presence of multipath reflections, employing sequential transmission of multiple frequencies in a slow-time (pulse-to-pulse) approach. First, we develop a parametric measurement model that accounts for the multipath components at multiple frequencies as well as Doppler shifts. Then, we develop a statistical detection test and analytically evaluate its performance characteristics. Based on the performance analysis, we propose an adaptive algorithm to select the best combination from a subset of frequencies that maximizes the detection performance. Our numerical examples show that the sequential approach requires more coherent pulses to match the performance of the simultaneous usage of multiple carriers in OFDM format. We also study the extent of performance degradation due to employing a subset of available frequencies.

Index Terms— Slow time, multi-frequency radar, multipath reflection, target detection, generalized likelihood ratio test.

I. INTRODUCTION

The problem of detection and tracking targets in the presence of multipath has been considered challenging in the radar community for many years. Conventional radar systems try to suppress the multipath reflections by treating them as interference (or clutter). However, a proper exploitation of multipath propagation can improve the radar performance [1], [2]. Each multipath component provides an extra "look" at the target and is affected by a different Doppler shift corresponding to the projection of the target velocity on the direction-of-arrival (DOA) vector, and thus improves the target detection capability.

To resolve and exploit the multipath components, in [2] we considered a wideband orthogonal frequency division multiplexing (OFDM) signalling scheme [3]. Although OFDM has been elaborately studied and commercialized in the digital communication field [4], it has not so widely been studied by the radar community apart from a few recent efforts [5]-[7]. One of major reasons of such unpopularity is that OFDM has a time-varying envelope and that originates a potentially high peak-to-average power ratio (PAPR) [8].

Over the years a number of approaches have been proposed to reduce the PAPR problem and a comprehensive survey of those techniques can be found in [8], [9, Ch. 6]. However, these techniques suggest modifications to the OFDM signal over "fast time" (within a pulse). Instead, here we propose to use a "slow-time" (pulse-to-pulse) approach in which only one of subcarriers (which certainly has constant envelope) is employed over a particular pulse. This approach is similar to the slow frequency-hop technique [10], in which different subcarriers are transmitted in a sequential manner instead of a simultaneous transmission as in OFDM.

In Section II, we develop the measurement model that accounts for the specular multipath reflections, under the generalized multivariate analysis of variance (GMANOVA) framework [11], [12]. Based on this model, in Section III, we formulate the detection problem and employ the generalized likelihood ratio (GLR) test [13, Ch. 6]. We analytically evaluate the performance the GLR test statistics under both hypotheses. In Section IV, we propose an adaptive design algorithm to select the best combination from a subset of frequencies that maximizes the detection performance. Numerical examples and conclusions are presented in Section V and VI, respectively. We find that for the same transmitting energy per pulse the sequential approach requires more coherent pulses to match the performance of its simultaneous version.

II. PROBLEM DESCRIPTION AND MODELING

We consider a far-field point target moving with a constant relative velocity $\boldsymbol{v}$ in a multipath-rich environment. At the operating frequency we assume that the reflecting surfaces only produce first-order specular reflections of the radar signal. We assume that for every range cell the radar knows the number of possible multipath (P) between the radar and target and the DOA unit-vectors ($\boldsymbol{u}_p,\, p = 0, 1, \ldots, P-1$) along each such path. Under this scenario, we first introduce the parametric measurement model for a sequential transmission of multiple frequencies. Then, we discuss our statistical assumptions on the noise and interference.

II-A. Measurement Model

We consider a radar operating with a bandwidth of B Hz and pulse duration of T seconds. It employs L different carrier frequencies, each of which can be represented as $s(t) = e^{\,j2\pi l(n)\Delta f t}$, where $l(n) \in \{0, 1, \ldots, L-1\}$ is the index of the carrier transmitted during the n-th pulse, $n = 0, 1, \ldots, N-1$ denote the slow-time indices, N is the number of temporal measurements within a given coherent processing interval (CPI), $\Delta f = 1/T = B/(L+1)$ (similar to the OFDM signal model of [2]), and t represents fast time.

Then, the complex envelope of the received signal corresponding to a specific range cell containing the target is given by

$$y(t) = \sum_{p=0}^{P-1} x_{l(n)p}\, e^{\,-j2\pi f_c \tau_p}\, e^{\,j2\pi l(n)\Delta f(t-\tau_p)}\, e^{\,j2\pi f_c \beta_p t} + e(t), \quad (1)$$

This work was supported by the Department of Defense under the Air Force Office of Scientific Research MURI Grant FA9550-05-1-0443 and ONR Grant N000140810849.

where $x_{l(n)p}$ is a complex quantity representing the scattering coefficient of the target along $l(n)$-th carrier and p-th path, τ_p and $\beta_p = 2\langle \boldsymbol{v}, \boldsymbol{u}_p \rangle / c$ are the roundtrip delay and Doppler shift, respectively, along the p-th path, c is the speed of propagation, and $e(t)$ is the additive measurement noise. Here we have implicitly assumed that all the multipath delayed signals from the target lie within the range cell under consideration. In addition, we assume that $|\tau_i - \tau_j| \ll \tau_0$ for $i, j = 0, 1, \ldots, P-1$. These assumptions can be justified in systems where the path lengths of multipath arrivals differ little (e.g., narrow urban canyon where the range is much greater than the width).

Moreover, the information of the roundtrip delays can be incorporated into the model by choosing $t = \tau + nT_{\text{PRI}}$, where T_{PRI} is the pulse repetition interval (PRI). Hence, noticing that $e^{j2\pi l(n)\Delta f n T_{\text{PRI}}} = 1$, we can simplify (1) to

$$y(n) = \boldsymbol{x}_{l(n)}^T \boldsymbol{\phi}(n, \boldsymbol{\eta}) + e(n), \tag{2}$$

where $\boldsymbol{x}_{l(n)} = \left[x_{l(n)0}, x_{l(n)1}, \ldots, x_{l(n)P-1}\right]^T$, $\boldsymbol{\phi}(n, \boldsymbol{\eta}) = e^{-j2\pi f_c \tau} \cdot \left[e^{j2\pi f_c \beta_0 \left(\tau + nT_{\text{PRI}}\right)}, \ldots, e^{j2\pi f_c \beta_{P-1}\left(\tau + nT_{\text{PRI}}\right)}\right]^T$, and $\boldsymbol{\eta}$ represents the unknown target-velocity components.

Now, suppose we opt for an ordered sequential transmission scheme in which the first carrier frequency is used in the first pulse, the second carrier frequency in second pulse, and so on. For example, with $L = 4$ we employ $l(n) = 0, 1, 2, 3$ for $n = 0, 1, 2, 3$, respectively. We repeat again in the same way stating with the first carrier frequency in $(L+1)$-th pulse. Thus, here we make a small assumption that N/L is a positive integer, which is very simple to implement. We concatenate all the temporal data columnwise into an $1 \times N$ row vector, keeping the similarity with [2, Eq. 5], to obtain the measurement model

$$\boldsymbol{y}^T = \boldsymbol{x}^T \boldsymbol{\Phi}(\boldsymbol{\eta}) + \boldsymbol{e}^T, \tag{3}$$

where $\boldsymbol{y} = [y(0), \ldots, y(N-1)]^T$, $\boldsymbol{x} = \left[\boldsymbol{x}_{l(0)}^T, \ldots, \boldsymbol{x}_{l(N-1)}^T\right]^T$, $\boldsymbol{\Phi} = \left[\boldsymbol{\Phi}_{0:L-1} \quad \cdots \quad \boldsymbol{\Phi}_{N-L-2:N-1}\right]$ with $\boldsymbol{\Phi}_{0:L-1} = \text{blkdiag}\left(\boldsymbol{\phi}(0, \boldsymbol{\eta}), \boldsymbol{\phi}(1, \boldsymbol{\eta}), \ldots, \boldsymbol{\phi}(L-1, \boldsymbol{\eta})\right)$.

Next, we choose a random sequential transmission scheme in which all the L carrier frequencies are used in the first L pulses in a random manner without any repetition. For example, with $L = 4$ we may have $\{l(n) = 2, 1, 3, 0\}$ for $n = 0, 1, 2, 3$, respectively. Then, for each of the next sets of L pulses we follow this same random transmission scheme. To incorporate this random scheme into (3) we need to post-multiply the scattering vector $\boldsymbol{x}$ with an $LP \times LP$ block-permutation matrix. For example, with the above-mentioned random scheme $\{l(n) = 2, 1, 3, 0\}$ we select the block-permutation matrix as

$$\boldsymbol{\mathcal{P}} = \begin{bmatrix} \boldsymbol{0} & \boldsymbol{0} & \boldsymbol{0} & \boldsymbol{I}_P \\ \boldsymbol{0} & \boldsymbol{I}_P & \boldsymbol{0} & \boldsymbol{0} \\ \boldsymbol{I}_P & \boldsymbol{0} & \boldsymbol{0} & \boldsymbol{0} \\ \boldsymbol{0} & \boldsymbol{0} & \boldsymbol{I}_P & \boldsymbol{0} \end{bmatrix}, \tag{4}$$

where $\boldsymbol{I}_P$ is an identity matrix of dimension P. Then, a modified form of (3) can be written as

$$\boldsymbol{y}^T = \boldsymbol{x}^T \boldsymbol{\mathcal{P}} \boldsymbol{\Phi}(\boldsymbol{\eta}) + \boldsymbol{e}^T = \boldsymbol{x}^T \widetilde{\boldsymbol{\Phi}}(\boldsymbol{\eta}) + \boldsymbol{e}^T, \tag{5}$$

where $\widetilde{\boldsymbol{\Phi}}(\boldsymbol{\eta}) = \boldsymbol{\mathcal{P}} \boldsymbol{\Phi}(\boldsymbol{\eta})$. (5) reduces to (3) when $\boldsymbol{\mathcal{P}} = \boldsymbol{I}_{LP}$.

II-B. Statistical Assumptions

We assume that $e(n)$ is temporally white and circularly symmetric zero-mean complex Gaussian random variable with unknown variance σ^2. Therefore, the measurements are distributed as

$$\boldsymbol{y}^T \sim \mathbb{CN}_{1,N}\left(\boldsymbol{x}^T \widetilde{\boldsymbol{\Phi}}(\boldsymbol{\eta}),\, \sigma^2 I_N\right). \tag{6}$$

III. DETECTION TEST

In this section, we first develop a statistical detection test for the model presented in Section II-A, and then we analytically derive the performance characteristics of the test. We construct the decision problem to choose between two possible hypotheses $\mathcal{H}_0$ (target-free hypothesis) and $\mathcal{H}_1$ (target-present hypothesis) as

$$\begin{cases} \mathcal{H}_0: & \boldsymbol{x} = \boldsymbol{0}, \quad \sigma^2 \text{ unknown} \\ \mathcal{H}_1: & \boldsymbol{x} \neq \boldsymbol{0}, \quad \boldsymbol{\eta}, \sigma^2 \text{ unknown} \end{cases} \tag{7}$$

Because of the lack of knowledge about $\boldsymbol{\eta}$ and σ^2 we use the generalized likelihood ratio (GLR) test [13, Ch. 6] in which the unknown parameters are replaced with their maximum likelihood estimates (MLE).

III-A. GLR Test

When the parameter $\boldsymbol{\eta}$ in (5) is known, the GLR test compares the ratio of the likelihood functions under the two hypotheses with a threshold as follows [13, Ch. 6.4.2]:

$$\text{GLR}(\boldsymbol{\eta}) = \frac{f_{\mathcal{H}_1}(\boldsymbol{y}; \boldsymbol{\eta}, \widehat{\boldsymbol{x}}, \widehat{\sigma^2}_1)}{f_{\mathcal{H}_0}(\boldsymbol{y}; \widehat{\sigma^2}_0)} \underset{>}{^{\mathcal{H}_1}} \gamma, \tag{8}$$

where $f_{\mathcal{H}_0}$ and $f_{\mathcal{H}_1}$ are the likelihood functions under $\mathcal{H}_0$ and $\mathcal{H}_1$, $\widehat{\sigma^2}_0$ and $\widehat{\sigma^2}_1$ are the MLEs of σ^2 under $\mathcal{H}_0$ and $\mathcal{H}_1$, $\widehat{\boldsymbol{x}}$ is the MLE of $\boldsymbol{x}$ under $\mathcal{H}_1$, and γ is the detection threshold. After some algebraic manipulations [12], it can be shown that $\widehat{\boldsymbol{x}}^T(\boldsymbol{\eta}) = \boldsymbol{y}^T \widetilde{\boldsymbol{\Phi}}(\boldsymbol{\eta})^H \left(\widetilde{\boldsymbol{\Phi}}(\boldsymbol{\eta}) \widetilde{\boldsymbol{\Phi}}(\boldsymbol{\eta})^H\right)^-$ and

$$\frac{1}{\text{GLR}(\boldsymbol{\eta})} = \frac{\boldsymbol{y}^T \boldsymbol{\Pi}_1(\boldsymbol{\eta}) \boldsymbol{y}^*}{\boldsymbol{y}^T \boldsymbol{\Pi}_1(\boldsymbol{\eta}) \boldsymbol{y}^* + \boldsymbol{y}^T \boldsymbol{\Pi}_2(\boldsymbol{\eta}) \boldsymbol{y}^*}, \tag{9}$$

where $\boldsymbol{\Pi}_1(\boldsymbol{\eta}) = \boldsymbol{I}_N - \boldsymbol{\Pi}_2(\boldsymbol{\eta})$ and $\boldsymbol{\Pi}_2(\boldsymbol{\eta}) = \widetilde{\boldsymbol{\Phi}}(\boldsymbol{\eta})^H \left(\widetilde{\boldsymbol{\Phi}}(\boldsymbol{\eta}) \widetilde{\boldsymbol{\Phi}}(\boldsymbol{\eta})^H\right)^- \widetilde{\boldsymbol{\Phi}}(\boldsymbol{\eta})$ are two projection matrices orthogonal to each other. In case of unknown $\boldsymbol{\eta}$, the GLR test compares $\max_{\boldsymbol{\eta}} \text{GLR}(\boldsymbol{\eta}) = \text{GLR}(\hat{\boldsymbol{\eta}})$ with a threshold.

III-B. Detection Performance

Under $\mathcal{H}_0$ and $\mathcal{H}_1$, we have $\boldsymbol{y}^T \sim \mathbb{CN}_{1,N}(\boldsymbol{0}^T, \sigma^2 \boldsymbol{I}_N)$ and $\boldsymbol{y}^T \sim \mathbb{CN}_{1,N}(\boldsymbol{\mu}^T, \sigma^2 \boldsymbol{I}_N)$, respectively, where $\boldsymbol{\mu}^T = \boldsymbol{x}^T \widetilde{\boldsymbol{\Phi}}(\boldsymbol{\eta})$. Therefore, it can be shown that $\boldsymbol{y}^T \boldsymbol{\Pi}_1 \boldsymbol{y}^*$ follows a complex central chi-square distribution with $(N - r)$ and r complex degrees of freedom under both the hypotheses, whereas $\boldsymbol{y}^T \boldsymbol{\Pi}_2 \boldsymbol{y}^*$ is distributed as a complex central and non-central chi-square distributions with the same degrees of freedom under $\mathcal{H}_0$ and $\mathcal{H}_1$, respectively. The non-centrality parameter is given by $\boldsymbol{\mu}^T \boldsymbol{\mu}^* / \sigma^2$. Furthermore, using the orthogonal complement property of the projection matrices (i.e., $\boldsymbol{\Pi}_1 \boldsymbol{\Pi}_2 = \boldsymbol{0}$) and Craig-Sakamoto theorem [14], [15], we have that $\boldsymbol{y}^T \boldsymbol{\Pi}_1 \boldsymbol{y}^*$ and $\boldsymbol{y}^T \boldsymbol{\Pi}_2 \boldsymbol{y}^*$ are independent. Hence, under $\mathcal{H}_0$ the GLR test statistic follows a complex central beta distribution with $N - r$ and r complex degrees of freedom, written as

$$\frac{1}{\text{GLR}(\boldsymbol{\eta})} \sim \mathbb{CB}(N - r,\, r), \tag{10}$$

and under $\mathcal{H}_1$ follows a complex non-central beta distribution with non-centrality parameter $\boldsymbol{\mu}^T\boldsymbol{\mu}^*/\sigma^2$, denoted as

$$\frac{1}{\mathrm{GLR}(\boldsymbol{\eta})} \sim \mathbb{CB}(N-r, r; \boldsymbol{\mu}^T\boldsymbol{\mu}^*/\sigma^2), \tag{11}$$

where $r = \mathrm{rank}[\widetilde{\boldsymbol{\Phi}}(\boldsymbol{\eta})] \leq LP < N$. Thus, when $\boldsymbol{\eta}$ is known, (9) also corroborates to a constant false alarm rate (CFAR) test; refer to [16, Ch. 4, 6] for the detailed derivations of (10), (11), and the subsequent analytical expressions of the probabilities of false alarm (P_{FA}) and detection (P_{D}).

IV. SELECTING FREQUENCY SUBSET

In this section, we develop an adaptive design technique to select the best combination from a subset of frequencies such that probability of detection is maximized. This could be critical in some radar applications where saving resources is one of the primary importance.

Suppose, the radar wants to use only $L-1$ carrier frequencies out of the L available frequencies (denoted as a set $\mathfrak{F}_L$). However, there are $\binom{L}{L-1} = L$ different ways to form a subset $\mathfrak{F}_{L-1}$ from the set $\mathfrak{F}_L$. To choose the best combination of $L-1$ frequencies we look into our discussions of the previous section. We note that the GLR test results in a CFAR detector when $\boldsymbol{\eta}$ is known and the detection performance depends on the system parameters through the non-centrality parameter $\boldsymbol{\mu}^T\boldsymbol{\mu}^*/\sigma^2 = \boldsymbol{x}^T\widetilde{\boldsymbol{\Phi}}(\boldsymbol{\eta})\widetilde{\boldsymbol{\Phi}}(\boldsymbol{\eta})^H\boldsymbol{x}^*/\sigma^2$.

To compute an equivalent non-centrality parameter associated with $\mathfrak{F}_{L-1}$, we first form a reduced version of the target scattering coefficients, $\boldsymbol{x}_{\mathrm{red},k}$, that ignores the responses corresponding to the k-th carrier frequency, as

$$\boldsymbol{x}_{\mathrm{red},k} = \widehat{\boldsymbol{x}}(\widehat{\boldsymbol{\eta}}) \odot \boldsymbol{m}_k \quad \text{for } k = 0, 1, \ldots, L-1, \tag{12}$$

where $\boldsymbol{m}_k = \left[\mathbf{1}_P^T, \ldots, \mathbf{1}_P^T, \mathbf{0}_P^T, \mathbf{1}_P^T, \ldots, \mathbf{1}_P^T\right]^T$ is a masking vector that has all the entries equal to 1 except for those corresponding to the k-th carrier frequency and $\odot$ is the element-wise Hadamard product. Then, we formulate the optimization procedure to choose the best combination of $L-1$ frequencies that maximizes the corresponding non-centrality parameter, i.e.,

$$\mathfrak{F}_{L-1}^{\mathrm{opt}} = \underset{\mathfrak{F}_{L-1}^k}{\mathrm{argmax}}\ \boldsymbol{x}_{\mathrm{red},k}^T\widetilde{\boldsymbol{\Phi}}(\widehat{\boldsymbol{\eta}})\widetilde{\boldsymbol{\Phi}}(\widehat{\boldsymbol{\eta}})^H\boldsymbol{x}_{\mathrm{red},k}^*/\widehat{\sigma^2}, \tag{13}$$

where $\mathfrak{F}_{L-1}^k$ is a subset of $\mathfrak{F}_L$ after eliminating the k-th carrier frequency.

Similarly, we can extend this procedure to ignore more than one carrier frequencies and choose the optimum combinations of frequencies, like $\mathfrak{F}_{L-2}^{\mathrm{opt}}$, $\mathfrak{F}_{L-3}^{\mathrm{opt}}$, etc. However, as we neglect more frequencies the performance of the detector will deteriorate. Hence, it calls for a compromise between the usage of lesser number of carrier frequencies and associated detector performance.

V. NUMERICAL RESULTS

In this section, we present the results of several simulations to illustrate our analytical results. For simplicity we consider a 2D scenario. The velocity of the target is assumed to be $\boldsymbol{v} = 10\hat{i} + 10\hat{j}$ m/s and it remains within a particular range cell throughout a given CPI. We simulated the situation of a range cell centered at 2 km North and 5m East with respect to the radar (positioned at the origin). We assumed that there exist three different paths (i.e., $P = 3$) between that particular range cell and the radar.

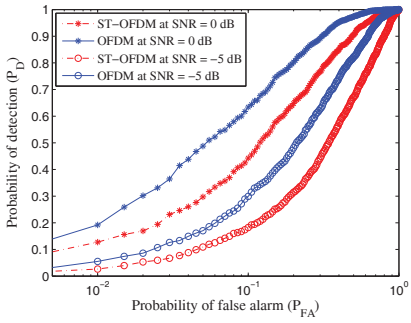

Fig. 1. Probability of detection as a function of probability of false alarm for different SNR values.

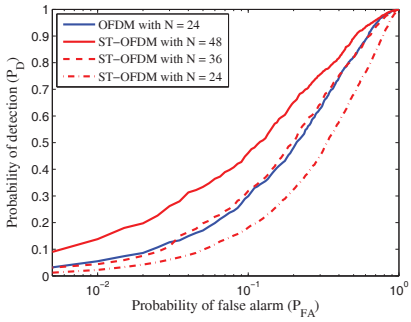

Fig. 2. Probability of detection as a function of probability of false alarm for different numbers of temporal samples.

We considered a radar operating with the following specifications: carrier frequency $f_{\mathrm{c}} = 1$ GHz; available bandwidth $B = 125$ MHz; number of carriers $L = 4$; spacing between the carriers $\Delta f = B/(L+1) = 25$ MHz; pulse width $T = 1/\Delta f = 40$ ns; pulse repetition interval $T_{\mathrm{PRI}} = 20$ μs; number of coherent pulses $N = 24$. We opted for an ordered sequential transmitting pattern (i.e., $\boldsymbol{\mathcal{P}} = \boldsymbol{I}_{LP}$). In this section, we refer the proposed approach as slow-time OFDM (ST-OFDM) as we compared its performance with that of the OFDM radar (proposed in [2]) having the same specifications. For a fair comparison of these two systems, we also kept fixed the transmitted energy per pulse by ensuring $a_l = 1/\sqrt{L}\ \forall l$ for the OFDM radar.

We performed Monte Carlo simulations based on $20,000$ independent trials to realize the following results. The entries of $\boldsymbol{x}$ were realized from a $\mathbb{CN}(0,1)$ distribution and σ^2 was chosen to satisfy the required signal-to-noise ratio (SNR), defined as

$$\mathrm{SNR} = (1/N)\sum_{n=1}^{N}\left|\boldsymbol{x}^T\widetilde{\boldsymbol{\phi}}(n, \boldsymbol{\eta}_{\mathrm{TRUE}})\right|^2/\sigma^2. \tag{14}$$

V-A. Detector Performance

Fig. 1 depicts the receiver operating characteristics (ROC), showing the variations of probability of detection (P_{D}) as a function of probability of false alarm (P_{FA}), of the ST-OFDM detector at two different SNR values. We compared its performance with that of the OFDM detector. It is evident that at a fixed SNR value the

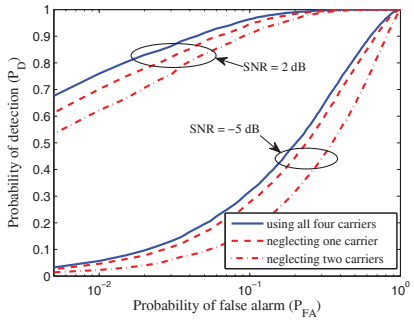

Fig. 3. Probability of detection as a function of probability of false alarm for different numbers of temporal samples.

wideband OFDM with simultaneous usage of multiple frequencies performs better than its narrowband sequential approach for the same transmitted energy per pulse.

However, the performance of the ST-OFDM detector improves when we have the possibility of obtaining more temporal samples. Fig. 2 shows the ROCs of the ST-OFDM detector at three different values of N, while keeping the SNR fixed at -5 dB. This shows that the ST-OFDM detector can perform similar to, or even better than, the OFDM detector if it can operate with a longer CPI. For example, in this simulation the ST-OFDM detector requires 50% more temporal samples to match the performance of the OFDM detector.

V-B. Employing a Subset of Frequencies

To study the extent of performance degradation due to employing a subset of available frequencies we devised the following simulation. We assumed a system that employs all the $L = 4$ carrier frequencies in the first N pulses. Based on the corresponding measurements we used (13) to compute which one of the L frequencies can be neglected with minimum performance loss, and then transmitted the rest $L-1$ carrier frequencies over the next N pulses. We compared this system with another system that transmits all the L carrier frequencies in the corresponding two sets of N pulses. Fig. 3 depicts the ROCs of these systems at two different SNR values. We observe that while operating at low SNR (e.g., SNR $= -5$ dB) the detection performance does not deteriorate much if we ignore one of the L frequencies. However, from Fig. 3 we also notice that the detector performance drops considerably when two of the L frequencies are neglected.

VI. CONCLUSIONS

In this paper, we addressed the problem of detecting a moving target by exploiting multipath reflections. We first introduced a parametric measurement model for a sequential slow-time transmission of multiple frequencies. Then, we formulated a hypothesis test to decide about the presence of a moving target in a particular range cell. We analytically evaluated the performance of this proposed detector. Based on the performance analysis, we proposed a design technique to choose the best combination from a subset of available frequencies that maximizes the detection performance. Our numerical examples show that the sequential transmission of multiple carriers requires more coherent pulses to match the performance of its simultaneous counterpart. In our future work, we will extend our model to incorporate more realistic physical effects, such as diffraction. We will integrate our detection procedure with target tracking algorithm and validate the performance of our proposed detector with real data.

VII. REFERENCES

[1] J. L. Krolik, J. Farrell, and A. Steinhardt, "Exploiting multipath propagation for GMTI in urban environments," in *IEEE Conf. on Radar*, 24–27, 2006, pp. 65–68.

[2] S. Sen, M. Hurtado, and A. Nehorai, "Adaptive OFDM radar for detecting a moving target in urban scenarios," in *International Waveform Diversity and Design Conference*, Orlando, FL, Feb. 8–13, 2009, pp. 268–272.

[3] A. Pandharipande, "Principles of OFDM," *IEEE Potentials*, vol. 21, no. 2, pp. 16–19, Apr. 2002.

[4] B. Le Floch, R. Halbert-Lassalle, and D. Castelain, "Digital sound broadcasting to mobile receivers," *IEEE Trans. Consum. Electron.*, vol. 35, no. 3, pp. 493–503, Aug. 1989.

[5] G. E. A. Franken, H. Nikookar, and P. Van Genderen, "Doppler tolerance of OFDM-coded radar signals," in *Proc. of the 3rd European Radar Conference*, Manchester, UK, Sept. 13–15, 2006, pp. 108–111.

[6] D. S. Garmatyuk, "Simulated imaging performance of UWB SAR based on OFDM," in *The IEEE 2006 International Conference on Ultra-Wideband*, Sept. 2006, pp. 237–242.

[7] J. P. Stralka, *Applications of Orthogonal Frequency-Division Multiplexing (OFDM) to Radar*, Ph.D. thesis, The Johns Hopkins University, Baltimore, MD, Mar. 2008.

[8] S. H. Han and J. H. Lee, "An overview of peak-to-average power ratio reduction techniques for multicarrier transmission," *IEEE Wireless Comm.*, vol. 12, no. 2, pp. 56–65, Apr. 2005.

[9] R. Prasad, *OFDM for wireless communications systems*, Artech House, June 2004.

[10] R. E. Ziemer, R. L. Peterson, and D. E. Borth, *Introduction to Spread Spectrum Communications*, Prentice Hall, Apr. 1995.

[11] R. F. Potthoff and S. N. Roy, "A generalized multivariate analysis of variance model useful especially for growth curve problems," *Biometrika*, vol. 51, no. 3/4, pp. 313–326, Dec. 1964.

[12] A. Dogandzic and A. Nehorai, "Generalized multivariate analysis of variance: A unified framework for signal processing in correlated noise," *IEEE Signal Process. Mag.*, vol. 20, pp. 39–54, Sept. 2003.

[13] S. M. Kay, *Fundamentals of Statistical Signal Processing: Detection Theory*, Prentice Hall PTR, Upper Saddle River, NJ, 1998.

[14] A. T. Craig, "Note on the independence of certain quadratic forms," *The Annals of Mathematical Statistics*, vol. 14, no. 2, pp. 195–197, June 1943.

[15] H. Sakamoto, "On the independence of two statistics," *Res. Mem. Inst. Statist. Math. Tokyo*, vol. 1, no. 9, pp. 1–25, 1944.

[16] E. J. Kelly and K. M. Forsythe, "Adaptive detection and parameter estimation for multidimensional signal models," Tech. Rep. 848, Lincoln Laboratory, MIT, Lexington, MA, Apr. 1989.